

The role of photon scattering in shaping the lightcurves and spectra of γ -ray bursts

Davide Lazzati

Institute of Astronomy, University of Cambridge, Madingley Road, Cambridge CB3 0HA, England
e-mail: lazzati@ast.cam.ac.uk

25 October 2018

ABSTRACT

We analyze the power spectra of the lightcurves of long gamma-ray bursts, dividing the sample in bins of luminosity, using the recently discovered variability-luminosity correlation. We find that the value of the variability parameter strongly correlates with the frequency that contains most of the power in the burst comoving frame. We compute the average power spectra in luminosity bins. The average power spectrum is well described by a broken power-law and the break frequency is a function of the variability parameter, while the two slopes are roughly constant. This allows us to conclude that scattering processes do not play a relevant role in modelling the lightcurves. We finally discuss in which conditions scattering may still play a relevant role in shaping the spectra of GRBs.

Key words: gamma-rays: burst

1 INTRODUCTION

The study of the BATSE γ -ray bursts (GRBs) lightcurves has recently gained new interest thanks to the discovery of the variability-luminosity (Fenimore & Ramirez-Ruiz 2000; Reichart et al. 2001) and lag-luminosity (Norris et al. 2000) correlations (see also Chang, Yoon & Choi 2002). These enable us to assign a tentative redshift to BATSE GRBs, allowing us to perform spectral and temporal analysis of the lightcurves in the burst comoving frame, where their properties are more closely linked to the physics of the burst itself. As an example, the use of these correlations enabled the possible discoveries of an evolution of the luminosity function with redshift (Lloyd-Ronning, Fryer & Ramirez-Ruiz, 2002) and of a correlation between the peak photon frequency with the luminosity of the GRB (Lloyd-Ronning & Ramirez-Ruiz 2002).

The variability-luminosity correlation predicts that the peak luminosity of a burst is correlated to its degree of variability, whose operational definition is related to the normalized variance, or the root mean square of the deviations from a smoothed version of the light curve. More variable lightcurves have larger luminosities. The lag-luminosity correlation is instead based on the measure of a temporal lag between the detection of high energy and low energy photons. It is found that the more the burst is luminous, the smaller is the lag. Besides being extremely useful tools, these correlations also call for an explanation of their origin. Several possible interpretations have been discussed in the literature. In particular, it is shown that an underlying correlation between the isotropic equivalent luminosity and the Lorentz factor of the fireball can explain both the corre-

lations (Ramirez-Ruiz & Lloyd-Ronning 2002; Kobayashi, Ryde & MacFadyen 2002; Salmonson 2000; Mészáros et al. 2002). In some of these works, however, a significant role is attributed to the modification of the temporal properties of the light curves as a consequence of scattering by cold or hot electrons (see also Panaitescu, Spada & Mészáros 1999; Spada, Panaitescu & Mészáros 2000). The role of scattering seems to be strengthened by the need of explaining the peak photon frequency vs. isotropic equivalent luminosity correlation (Lloyd-Ronning & Ramirez-Ruiz 2002), which is not naturally predicted in the internal shock scenario (Ghisellini, Celotti & Lazzati 1999).

In this paper, we concentrate on the variability luminosity correlation, using power spectra as a diagnostic to investigate several related issues. First (§2), we compute the dominant frequency of the power spectrum for each GRB in our sample of 220 lightcurves. We find that this dominant frequency strongly correlates with the variability measure. We then divide the sample in bins of variability and compute the average power spectrum. We find (§3) that the power spectra are self-similar (Beloborodov, Stern & Svensson 1998; 2000; hereafter B98 and B00; Chang & Yi 2000) in all the variability bins, with a break at a frequency that correlates with the variability parameter. No sign of a cut-off in the spectrum at large frequencies is observed. We (§4) develop a shot-noise model for the lightcurve, taking into account the effect of scattering in Fourier space (§5). In §6 we discuss our results, showing how scattering processes cannot be responsible for the variability-luminosity correlation, and also constraining the regions of the parameter space where

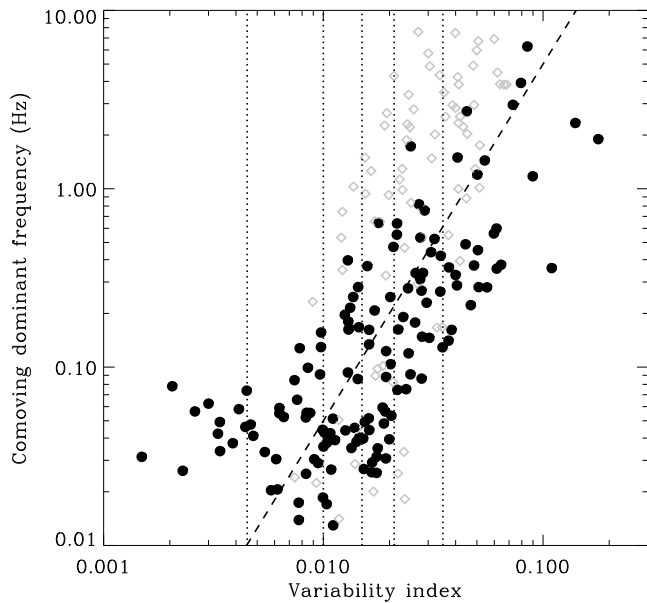


Figure 1. The dominant frequency in the burst comoving frame vs. the burst variability parameter. Solid points show the best class events (see Sect. 2 for details) while gray symbols show the lower class events. A correlation is clearly evident. The dashed line shows a relation $\nu_d \propto V^2$ as a guideline for the first class events. Vertical dotted lines show the boundaries of the subclasses in which the sample has been divided.

photon scattering on cold electrons may imprint detectable signatures on the photon spectra of GRBs without leaving a detectable trace in their power spectra.

2 DATA ANALYSIS

We have adopted the whole sample of GRBs for which Fenimore & Ramirez-Ruiz (2001) computed the variability parameter and a tentative redshift. For each lightcurve, we have computed the power spectrum (hereafter PSD) as $PSD(\nu) = |\tilde{f}(\nu)|^2$, where $\tilde{f}(\nu)$ is the Fourier transform of the lightcurve. Lightcurves were binned to 64 ms resolution and considered from the BATSE trigger time for a total duration of $t = 3 * T_{90}$, where T_{90} is the time containing 90% of the total burst emission. A cubic function was fitted to the time interval before and after the one considered above in order to remove the background. The effect of background removal was however weak, affecting only the smallest frequencies.

The dominant frequency ν_d was detected as the frequency at which the power per unit decade frequency is maximized (something similar to the peak of the $\nu F(\nu)$ photon spectrum), i.e. the maximum of the function $\nu PSD(\nu)$. We adopted this definition since it does not involve any fitting procedure and is therefore the most objective. The definition of the dominant frequency must confront, however, with two problems. First, we must consider that the time series is limited (see below), secondly the presence of a white noise component, which is due to the Poisson noise of the lightcurve (which is inevitably affected by photon count statistics). This component results in a flat power spectrum (see e.g. Leahy et al. 1983 and references therein) which produces

a false peak at the highest considered frequency when the $\nu PSD(\nu)$ function is considered for lightcurves in which the signal is weaker than a certain threshold. In order to avoid this contamination of spurious peaks, the spectra were all visually inspected, and every time the peak frequency was in the flat part of the PSD, the considered frequency range was shrunk in order to recompute the maximum in a shorter frequency range, where the signal-to-noise ratio is larger. This procedure, unavoidably, reduces the objectivity of the analysis, and for this reasons the lightcurves in which the peak selection was modified by hand were flagged. In Fig. 1 we show the comoving frame dominant frequency vs. the variability parameter for all the best class lightcurves, in which human intervention was either not required or clearly unbiased. A clear correlation is present. The correlation, according to the correlation coefficient statistics, is highly significant, with a vanishing probability of being spurious $P = 3 \times 10^{-25}$. It may be argued that the correlation is artificially made by a correlation between the redshift and the variability (which is indeed present in the data). In order to test for this to be true, we computed the above probability also for the observed frame frequency. Again, a strong correlation is found, with probability of being spurious $P = 8 \times 10^{-12}$. The lower class bursts, in which human intervention was necessary and possibly biased, or in which the dominant frequency was the lowest one, are plotted in light gray in Fig. 1. It is possible to see how these points do not invalidate the correlation, even though the dominant frequencies tend to be, as expected, larger than for the best cases. In the following we will perform our analysis only on the subsample of 143 best lightcurves shown in Fig. 1, even though extending it to the whole sample does not affect significantly the conclusions. It is worth stressing that such a correlation is not entirely surprising, since it simply says that the variability parameter has something to do with the mean frequency over the PSD. What is relevant, as we are going to discuss in much more detail in the following, is that this correlation tells us that a change in the variability parameter V reflects a change in the whole PSD rather than the suppression of high (or low) frequency power.

When computing the PSD of an experimental time series, one has to take into account all the effects due to the data binning and to the finite duration of the data. In particular for GRBs, this second issue is particularly tricky, since the data are truncated not by hand, but by the intrinsic duration of the event. Consider an infinite function $f_\infty(t)$. The binning process can be modelled as the convolution with a square filter $b(t)$ and the multiplication with a lattice $s(t)$ (a series of Dirac δ functions) with spacing equal to the full width of the square filter. The truncation of the data is represented as the multiplication with a window function $w(t)$ which is usually assumed to be the characteristic function of the considered interval, but may have different shapes in the case of GRBs (see below). Thanks to the properties of multiplication and convolution in Fourier space, the Fourier transform of f can be written as (Lazzati & Stella 1997; hereafter LS97):

$$\tilde{f}(\nu) = \{ [\tilde{f}_\infty(\nu) * \tilde{w}(\nu)] \tilde{b}(\nu) \} * \tilde{s}(\nu) \quad (1)$$

where the symbol $*$ indicates a convolution. Let us analyze the implications of Eq. 1 from right to left. The Fourier transform of the lattice of spacing δt (in our case

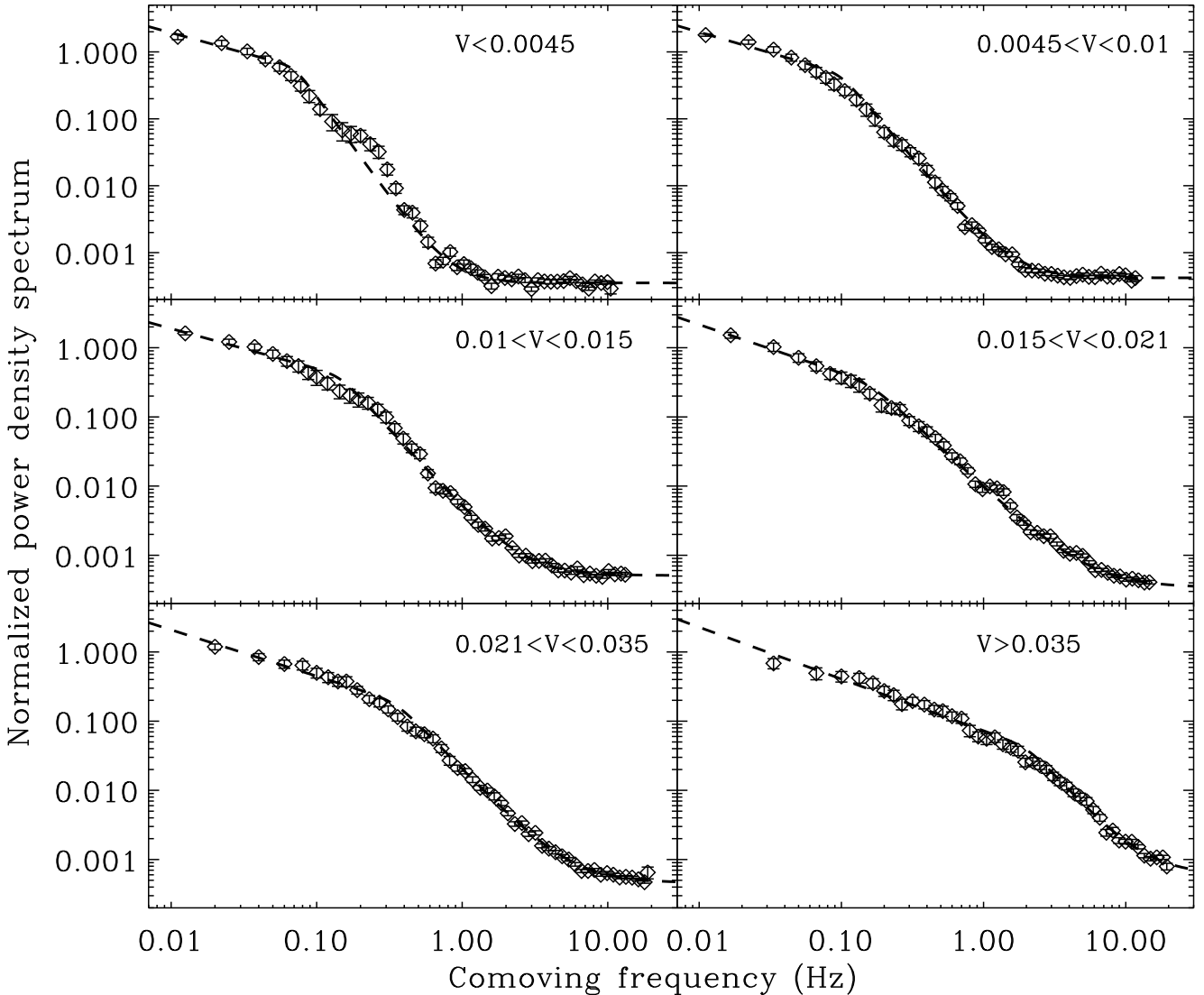


Figure 2. Average power spectra of burst in the six variability subclasses defined in the text (see also Fig. 1). The spectra have been binned in frequency in order to have a constant number of points per logarithmic unit frequency. The gray line shows the best broken power law (plus constant) fit. Error bars are derived from the dispersion of the sample.

64 ms) is the reciprocal lattice, i.e. a lattice with spacing $2\pi/\delta t \sim 100$ s. This term is important if periodicities are present in the lightcurve, since it gives rise to the well known phenomenon of aliasing. In our case, since the power spectra are monotonically decreasing with frequency, it is irrelevant. The Fourier transform of the binning function has a form (see, e.g., LS97)

$$\tilde{b}(\nu) \propto \frac{\sin(\pi \delta t \nu)}{\pi \delta t \nu} \quad (2)$$

This is the most dangerous term, since it introduces a break at a frequency $\nu \sim 1/\delta t \sim 16$ Hz in the observer frame. The largest of our dominant frequencies, in the observer frame, is $\max(\nu_d) = 0.5$ Hz. We conclude that this effect does not play a relevant role in our analysis. Finally, the effect of the window function is to smooth the observed PSD. In the most common case of a square function, the smoothing kernel is similar to the function in Eq. 2 but with a smaller width. Again, this term is important is small scale features overlaid

on the spectrum are concerned. For any reasonable shape of the window function we can ignore its effect.

We therefore conclude that the correlation of Fig 1 is real. It is worth noting that the typical frequencies, that seem to dominate the determination of the variability parameter V , are small, even in the comoving frame. This suggests that it is the ~ 1 second variability which is physically linked to the luminosity of the GRB rather than its shorter time scale fluctuations (see also below). There is also a suggestion, in the data, that the very small V bursts belong to a different family in terms of their temporal properties. We will discuss this in the following, finding that the average power spectra seem to be more consistent with a continuation of the average spectral properties rather than with a different subclass.

$\langle V \rangle$	α_1	α_2	ν_0 (Hz)	Prob(σ)
0.0032	0.6 ± 0.18	$3. \pm 0.15$	0.071 ± 0.016	7.2
0.0077	0.62 ± 0.1	2.5 ± 0.1	0.098 ± 0.017	> 8.3
0.0125	0.58 ± 0.09	2.3 ± 0.08	0.145 ± 0.03	> 8.3
0.018	0.7 ± 0.13	1.9 ± 0.06	0.16 ± 0.04	8.1
0.027	0.67 ± 0.09	2.16 ± 0.07	0.35 ± 0.07	> 8.3
0.053	0.75 ± 0.08	2.22 ± 0.3	2.0 ± 0.6	8.2

Table 1. Results of the fit of the average power spectra in Fig. 2. The rightmost column show the significance for the existence of the break.

3 AVERAGE POWER SPECTRA

We have divided the sample of 143 GRBs in six bins of the variability parameter V . Each bin contains ~ 25 lightcurves, with the exception of the smallest V bin, in which only 12 lightcurves are contained. This difference is due to the need of keeping these bursts isolated since they seem to belong to a different class. The lightcurves, background subtracted, were normalized to contain the same numbers of photons and the power spectra averaged at the same comoving frequency. The errors were derived from the dispersion of the sample.

This process is similar to what was done by B98 and B00. Their average power spectrum presents however three fundamental differences. First, they performed the average at the same observed frequency, instead of the comoving frequency. This was due to the fact that redshift estimates were not available at that time. Secondly, they decided to normalize their lightcurves to the same peak photon luminosity rather than to the same photon fluence. We decided to use this second normalization since the scatter in the sample of spectra was lower in this case (see B98 for a discussion). Finally they built the average of all the lightcurves, while we subdivide our sample in bins of variability.

The resulting average power spectra are shown in Fig. 2. The variability parameter increases from left to right and from top to bottom. The spectra seem to be made by a broken power law, sinking into the white noise at large frequencies. It is worth to note that our normalization criterion does not produce uniform white noise values. For this reason the subtraction of this component from the average spectra is not possible, and it is also dangerous to investigate the frequency region where the average spectra are dominated by white noise.

We fit the average spectra with smoothly a broken power-law function of the form

$$PSD(\nu) = \frac{2F_0}{\left[\left(\frac{\nu}{\nu_0} \right)^{2\alpha_1} + \left(\frac{\nu}{\nu_0} \right)^{2\alpha_2} \right]^{1/2}} + K \quad (3)$$

where α_1 is the slope at frequencies smaller than the break ν_0 , α_2 is the slope at larger frequencies and K is a constant that takes into account the contribution of the white noise. F_0 is the value of the PSD at the break frequency.

The results of the fit are reported in Tab. 1 and in Fig. 3. Several interesting remarks can be derived from the results. First, all the power spectra are well fit by the model. Moreover, the slopes of the broken power-law before and after the break are roughly consistent with being constant, with the break frequency ν_0 being the only quantity that evolves with

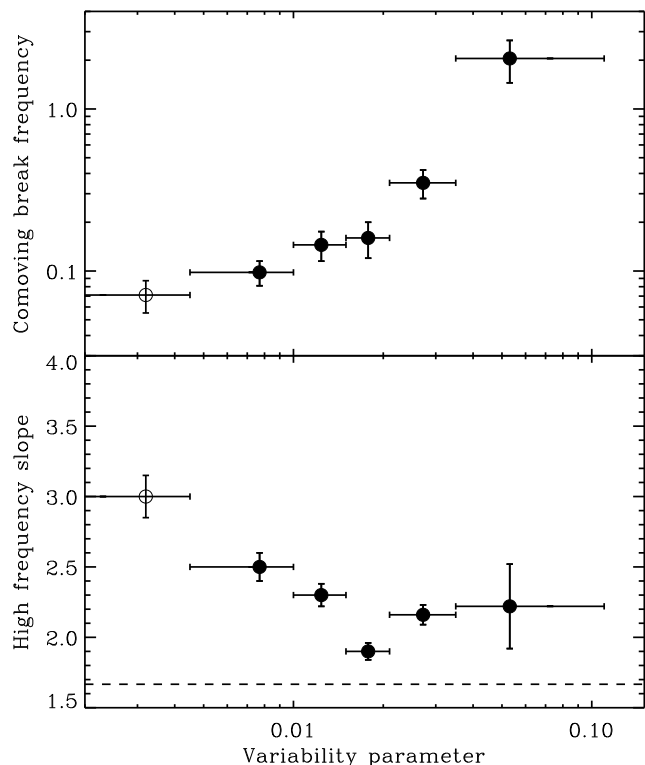


Figure 3. The break frequency and high energy slopes of the average power spectra versus variability. The upper panel shows the knee frequency as a function of variability. The first point (open circle) is for the lowest variability class. The lower panel shows the high frequency spectral index versus the variability parameter.

the variability parameter V . A marginal evidence of evolution of the high frequency power law index is also present, especially if the smallest variability bin is included in the sample. A second important remark is that the high frequency slope is larger than what found by B98. This difference is not due to the redshift correction nor to the different normalization. In fact, if we average among them the six power spectra of Fig. 6, we recover with good accuracy the $-5/3$ slope in B98. It looks therefore like that the slope can be attributed to the convolution of the break frequencies in different variability bins. Finally, even though the lowest variability bin values are different from the rest of the sample, it is not possible to define it as a separate class given the present data. The apparent segregation of the dominant frequencies in Fig. 1 may be due to the fact that the dominant frequencies of the very low variability bursts approach the lower cut in the analyzed frequencies, and include therefore an additional noise term.

4 SHOT NOISE MODEL

In the internal shock model for GRBs (Rees & Mészáros 1994) the lightcurve is modelled as the random superposition of a number of pulses with similar shape stretched in shape and scaled in luminosity according to some prescription for the ejection of shells by the inner engine (Kobayashi Sari & Piran 1997; Panaitescu et al. 1999;

Spada et al. 2000, 2001; Ramirez-Ruiz & Lloyd Ronning 2002). This lightcurve is similar to the shot noise model supposed to play a relevant role in the red-noise component observed in the power spectra of X-ray pulsars (LS97 and references therein).

Consider a normalized pulse of shape $p(t - t_0, \tau_r)$, with rise time τ_r and unit decay time and fluence peaking a time t_0 . A GRB lightcurve can be described as a random superposition of N such pulses:

$$lc(t) = \sum_j f_j p\left(\frac{t - t_j}{\alpha_j}, \tau_r\right) \quad (4)$$

where the pulse fluence f_j , the stretching factor α_j and the peak time t_j are randomly selected according to some prescription (for example simulating the hierarchical shock evolution of an inhomogeneous flow). The Fourier transform of the above equation can be written (up to a normalization factor) as:

$$\tilde{lc}(\omega) \propto \sum_j \tilde{f}(\alpha_j \omega) e^{-i\omega t_j} \quad (5)$$

When we compute the average power spectrum of a sample of lightcurves, under the assumption that each lightcurve is a random realization of the same underlying process, we compute the ensemble average of the square of the modulus of Eq. 5. This, if the peak times of the pulses are not correlated with their properties and are uniform in time¹, is given by (LS97):

$$\langle PSD \rangle \propto \langle \tilde{f}^2(\alpha\omega) \rangle \quad (6)$$

i.e. the average power spectrum is independent on the time history of the pulse ejection and on the pulse fluence distribution, but depends on the distribution of the pulse durations. To understand the effect of the above conclusion, we consider a simplified exponential pulse profile:

$$p(t) = e^{-t} \chi_{(0, \infty)} \quad (7)$$

where $\chi_{(a, b)}$ is the characteristic function of the interval (a, b) . In addition, we consider a power-law distribution² of α values between a minimum value α_m and a maximum value α_M :

$$n(\alpha) \propto \alpha^a \chi_{(\alpha_m, \alpha_M)} \quad (8)$$

The power spectrum of the single pulse of Eq. 7 is a Lorentzian function, i.e. (roughly speaking) a constant for $\nu < 1/2\pi$ and a power-law ν^{-2} for $\nu > 1/2\pi$. For the

¹ It is a well known result that the average width of the pulses does not evolve during the bursts (Ramirez-Ruiz & Fenimore 2000), but their frequency and/or fluence may be larger in the early phase of bursts. This correlations takes the form of a non-square window function in Fourier space, and are not relevant here, as discussed in § 2. Finally, it may be wrong to assume that the pulse fluence does not depend on the pulse duration (Ramirez-Ruiz & Fenimore 2000). Should this assumption be wrong, it would reflect in a different numeric value for Eq. 16.

² It has been found that the duration distribution of “well separated” pulses is well described by a Log-normal function (McBreen et al. 1994; Li & Fenimore 1999). We prefer to adopt a power-law distribution here since it fits better our average power-spectra and since our PSDs do include *non well separated* pulses.

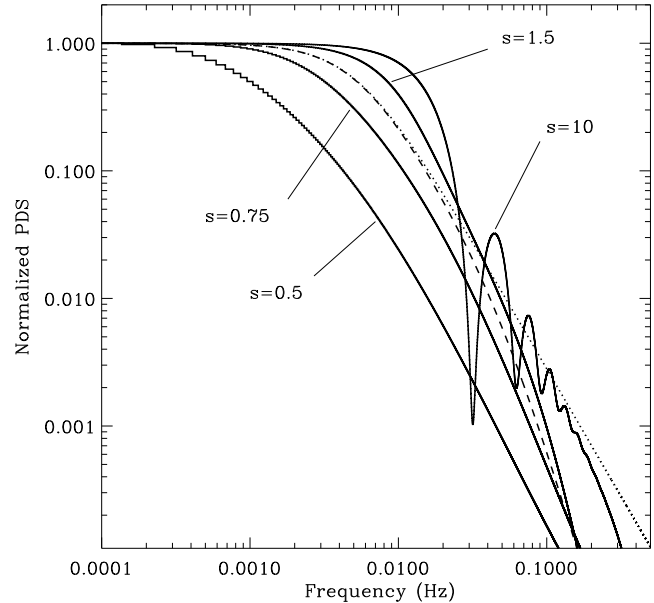


Figure 4. Power spectra for stretched exponential pulses as defined in Eq. 12, for the set of parameters $\tau_r = 3$ s, $\tau_d = 30$ s, and the values of s indicated. The dotted line shows the power spectrum for a single exponential profile while the dashed line shows the PSD for a double sided exponential profile.

stretched pulse, the PSD is flat for $\nu < 1/(2\pi\alpha)$ and a power law afterward. Consider now the average PSD of Eq. 6 for the α distribution defined in Eq. 8. If $a \leq -1$ the PSD will be dominated by the shortest pulse, and will retain a Lorentzian shape. For $a \geq 1$, it will be dominated by the longest pulse, again retaining the Lorentzian shape. For $-1 < a < 1$, a new power-law branch will appear, in the range $1/(2\pi\alpha_M) < \nu < 1/(2\pi\alpha_m)$, with a slope $\nu^{-(a+1)}$. Since for $a \geq 1$ the PSD is dominated by the longest pulse, here and in the following we will define the “shortest relevant pulse” as the shortest pulse that have an influence in the PSD shape. This pulse may not be the shortest observed in the lightcurve. For example, consider a broken power-law distribution of pulse durations, with $-1 < a < 1$ at short durations and $a \geq 1$ at short durations. the break in the power spectrum will be related to the pulse at the break of this distribution. We call this the shortest relevant pulse.

The shape of the fundamental pulse in Eq. 7 can be made more complicated. Consider as an example, a double exponential pulse, of functional shape:

$$p(t, \tau_r, \tau_d) = \frac{1}{\tau_r + \tau_s} \left[e^{\frac{t}{\tau_r}} \chi_{(-\infty, 0)} + e^{-\frac{t}{\tau_d}} \chi_{(0, +\infty)} \right] \quad (9)$$

Its PSD can be written as:

$$|\tilde{p}(\omega)|^2 \propto \frac{1}{1 + \omega^2 \tau_d^2 (\omega^2 \tau_r^2 + 1 + \tau_r^2 / \tau_d^2)} \quad (10)$$

where $\omega \equiv 2\pi\nu$ is the pulsation. If $\tau_r \ll \tau_d$, Eq. 10 can be approximated as a double broken power-law:

$$|\tilde{p}(\omega)|^2 \propto \begin{cases} \nu^0 & \nu \ll 1/2\pi\tau_d \\ \nu^{-2} & 1/2\pi\tau_d \ll \nu \ll 1/2\pi\tau_r \\ \nu^{-4} & \nu \gg 1/2\pi\tau_r \end{cases} \quad (11)$$

Again, the ensemble average of Eq. 6 can add different power-law branches if $-2 < a < 0$. Finally let us consider

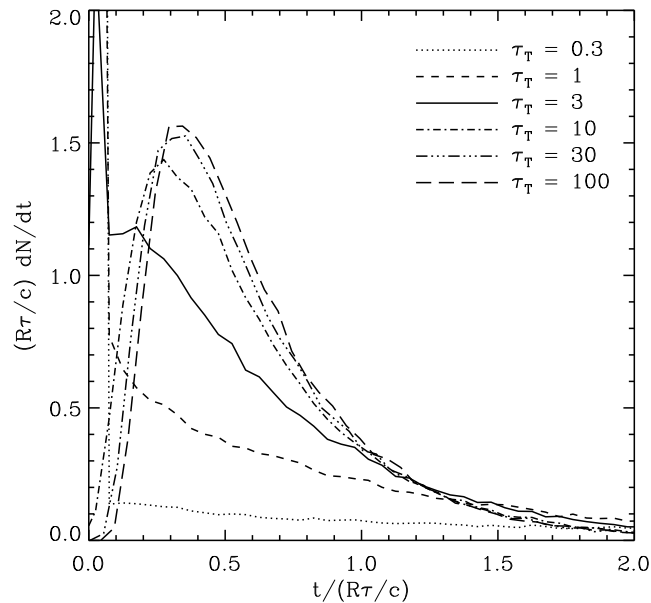


Figure 5. Transfer function shapes for a uniform cloud of perfect scattering centers with radius R and opacity τ_T . Different line styles show different opacities. For $\tau_T \gg 10$ the shape of the transfer function becomes scale invariant. Each curve is obtained by a Monte Carlo simulation with 10^5 input photons.

a stretched double exponential (Norris et al. 1996) of equation:

$$p(t, \tau_r, \tau_d) \propto \left[e^{\left(\frac{t}{\tau_r}\right)^s} \chi_{(-\infty, 0)} + e^{-\left(\frac{t}{\tau_d}\right)^s} \chi_{(0, +\infty)} \right] \quad (12)$$

For $s < 1$ this gives a pulse with a very spiky core and broad wings, while for $s > 1$ the resulting pulse has a square shape. The PSD cannot be analytically computed. In Fig. 4 we show the shape of the PSD for a set of values of s , compared to the PSD of the single and double exponential pulses. For $s < 1$ the effect is of smoothing out the breaks and extending the power-law branch ν^{-2} , while the effect of $s > 1$ is more complex. For $1 < s < 2$ the break frequency is moved to larger values, while the slope of the power-law decay is increased. For $s > 2$ the PSD starts to deviate from the simple form, with the appearance of “absorptions”. In an ensemble average these small scale features will be erased and we are left with the envelope, which yields again a very steep power-law slope.

5 PHOTON SCATTERING

It has been proposed that photon scattering may play a relevant role in shaping both the temporal (Panaitescu et al. 1999; Spada et al. 2000; Kobayashi et al. 2002; Ramirez-Ruiz & Lloyd-Ronning 2002) and spectral (Mészáros & Rees 2000, Mészáros et al. 2002) properties of GRB lightcurves. The effect of photon scattering has a distinctive signature in Fourier space, and the power spectrum of the lightcurves is then the best way in which the importance of scattering can be evaluated.

Consider a source of photons producing a flash (ideally a Dirac δ function in time) in the centre of a cloud of ideal

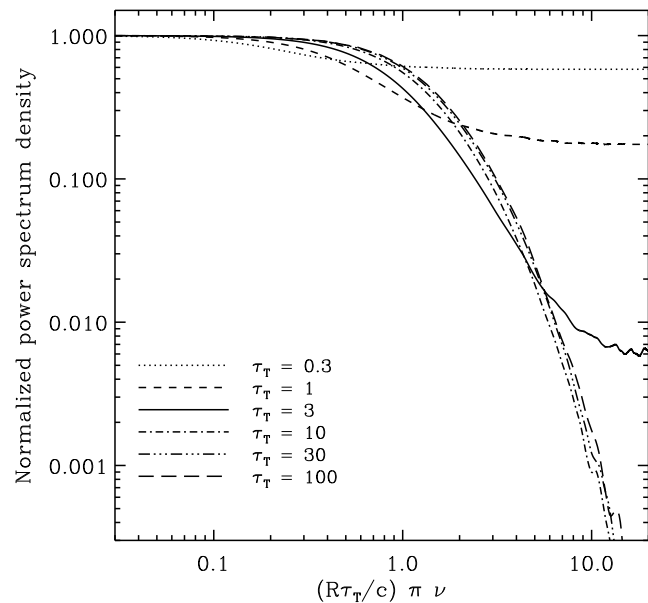


Figure 6. Power spectral density (normalized to the value at zero frequency) of the transfer functions shown in Fig. 5, as a function of the dimensionless frequency $(R\tau_T/c)\pi\nu$. For $\tau_T > 1$ the PSDs show a prominent break at the unit value of the dimensionless frequency.

scattering particles³. Even though the central source emitted a photon impulse, an observer located outside the cloud would detect a light pulse with a finite duration and a particular shape. This is due to the fact that different photons make different paths, finally reaching the observer after being scattered many times in random directions. The shape of this pulse will be function of the opacity of the cloud to photon scattering only, up to a scale factor that takes into account the size of the cloud.

Consider now the central source itself producing a signal with finite duration and with a given shape $s(t)$. This can be approximated as an infinite series of spikes, each of them being detected by the outside observer as a pulse of shape $k(t)$. In mathematical terms, the observer will detect a signal $S(t)$ given by the convolution of the original function $s(t)$ times the transfer function $k(t)$:

$$S(t) = s(t) * k(t) \equiv \int_{-\infty}^{\infty} s(t-t')k(t')dt' \quad (13)$$

Thanks to the properties of Fourier transforms, the PSD of the detected signal S is the product of the spectra of s and k .

In the case of photon scattering by free electrons, we consider a cloud of radius R and uniform density n , with opacity $\tau = Rn\sigma_T$. We neglect the angular dependence of the Thompson cross section. In Fig. 5, we show the transfer functions obtained by Monte-Carlo calculations of scattering for a set of optical depths. For $\tau \leq 1$ the transfer functions are Dirac δ function with a small tail at large times, but for $\tau > 1$ the vast majority of photons undergo at least

³ Ideal means in this context, that the photons are never absorbed and that the scattering properties of the cloud do not depend on the photon energy.

one scattering and the transfer function becomes much more smooth. For $\tau > 10$ the opacity itself is not a parameter any more but a scale factor:

$$k_{\tau > 10, \frac{R}{c}}(t) = \frac{c}{R\tau} k_{10,1} \left(\frac{ct}{R\tau} \right) \quad (14)$$

This behavior is reflected by the shape of the transfer functions in Fourier space. In Fig. 6 we show the PSD of the same transfer functions shown in Fig. 5. For small opacity, as expected, the PSD of the transfer function is almost a unit constant, so that $\tilde{S}(\omega) \simeq \tilde{s}(\omega)$. As the opacity increase, a pronounced break appears at a frequency

$$\nu_b = \frac{c}{\pi R \tau} \quad (15)$$

For intermediate opacities, the PSD can be roughly described as a power-law for $\nu > \nu_b$ while for large opacity the break takes the form of an exponential cutoff. In conclusion, the effect of photon scattering is to create a clear break in the power spectrum, suppressing all the frequencies larger than ν_b . In Fig. 7 we show the result of a set of simulations that include scattering at various degrees. The left column shows simulated lightcurves with a single exponential shot noise model (Eq. 7) with 20 pulses. The pulse fluence has a log-normal distribution, while the pulse duration τ_d is distributed according to Eq. 8 with $a = -1/2$, $\alpha_m = 10$ s and $\alpha_M = 250$ s. The top lightcurve has no scattering, while the second has $\tau = 3$ and the third has $\tau = 10$. In all cases $R/c = 1$. The last curve has been made by smoothing with $\tau = 10$ only the 7 shortest pulse. This may simulate more closely the effect of scattering in the internal shock scenario, where shorter pulses are produced closer to the inner engine, where the opacity of the flow is larger (see, e.g., Spada et al. 2001 and references therein). The second column shows the PSD of the lightcurves shown in the first column, while the third column shows the average PSD of 100 curves generated according to the same pulse process. The difference between the scattered and unscattered PSDs is shown by overlaying the unscattered PSD with a light grey curve.

As mentioned above, the effect of photon scattering in defining the duration of GRB pulses has been considered in a number of works (Panaitescu et al. 1999; Spada et al. 2000; Kobayashi et al. 2002; Ramirez-Ruiz & Lloyd-Ronning 2002). It is worth mentioning, however, that the way in which this was done is not completely accurate, especially when the power spectrum is concerned. In fact, in numerical works, the duration of a pulse is computed as the sum in quadrature of the intrinsic duration (due to the shell width and the angular spreading times) plus the scattering duration. This total duration is then used as a scale parameter for the pulse duration (the same as α in Eq. 4), assuming a fixed functional shape for the pulse⁴. On the contrary, when the diffusion time scale is comparable to or larger than the intrinsic time scale, the shape of the pulse should be changed, smoothing out its sharp features but leaving the long time scale features unaffected. When simulated lightcurves are observed in Fourier space, in both cases one has as expected that the average frequency has decreased. However, the real

scattering decreases the mean frequency by suppressing the high frequencies, while the above approximation rescales the whole spectrum at smaller frequencies. The result is that, while real scattering produces a prominent break in the spectrum, this approach leaves the spectral shape unaffected.

6 DISCUSSION

How do the shot-noise theory compares to the average spectra derived in § 3? The observed spectra show a clear break, which we show is strongly correlated with the variability parameter. The power-law slope changes from $-2/3$ before the break to ~ -2 after the break.

Let us for the moment neglect photon scattering. The fact that the largest slope is ~ -2 suggests that an exponential shot noise model can easily reproduce the observations, with a typical pulse decay time longer than the rise time (Norris et al. 1996). The fact that the low frequency slope is not flat, can be easily accommodated invoking a power-law distribution of pulse durations (cfr. Eq. 8)

$$n(\tau_d) \propto \tau_d^{-1/3} \quad (16)$$

The correlation between the break frequency and the variability (or the GRB luminosity) can therefore be interpreted as a correlation between the typical shortest relevant pulse duration and the luminosity. This does not mean that the lightcurve cannot have shorter pulses. In fact, if the distribution of pulse durations has a break, shorter pulses can be present but not contribute to the PSD.

Let us now consider the effect of photon scattering. In a very simple scenario, all the pulses may go through a scattering screen with opacity τ and radius R . In this case, a clear break should be present in the PSD at a frequency $\nu = c/(\pi R \tau)$. It is straightforward to show that the observed break cannot be due to scattering but must, instead, be attributed to the intrinsic properties of the unscattered pulses. In fact, the change of slope before and after the break is only of unity, while scattering would require either a jump of 2 in slope (intermediate opacity) or an exponential cutoff ($\tau > 10$). Alternatively, one can consider a scenario in which the opacity and size of the screen are different for different pulses. In order to be consistent with the lack of a pronounced break in the observations, this requires that the scattering time scale $\tau R/c$ is smaller than τ_d . In this case, the PSD of the single pulse would be affected only in the power-law tail and its effect would not be observed in the average PSD. In order to explain the break in the average PSD, however, one should consider a broken power-law of pulse durations. With such conditions one can explain the observed average power-spectrum. However, the role of scattering is not relevant in the shape of the PSD, and so it cannot be important in the measure of the variability parameter V . It may be also envisaged a case in which $\tau R/c \gg \tau_d$ for all pulses, with a broken power-law distribution of the values of τR suited to mimic the average PSD shape. In this case, however, the lightcurve would be entirely dominated by scattering. The pulses should have the shape of the transfer functions $k(t)$, in contradiction with what is found in their direct analysis (Norris et al. 1996).

A more detailed modelling of an internal shock process should however take into account that different pulses may

⁴ The approach of Kobayashi et al. (2002) was indeed different, in fact they assumed that all the collision between Thomson thick shells, typically those dominated by diffusion, do not produce any emission but reconvert the internal energy to outflow motion.

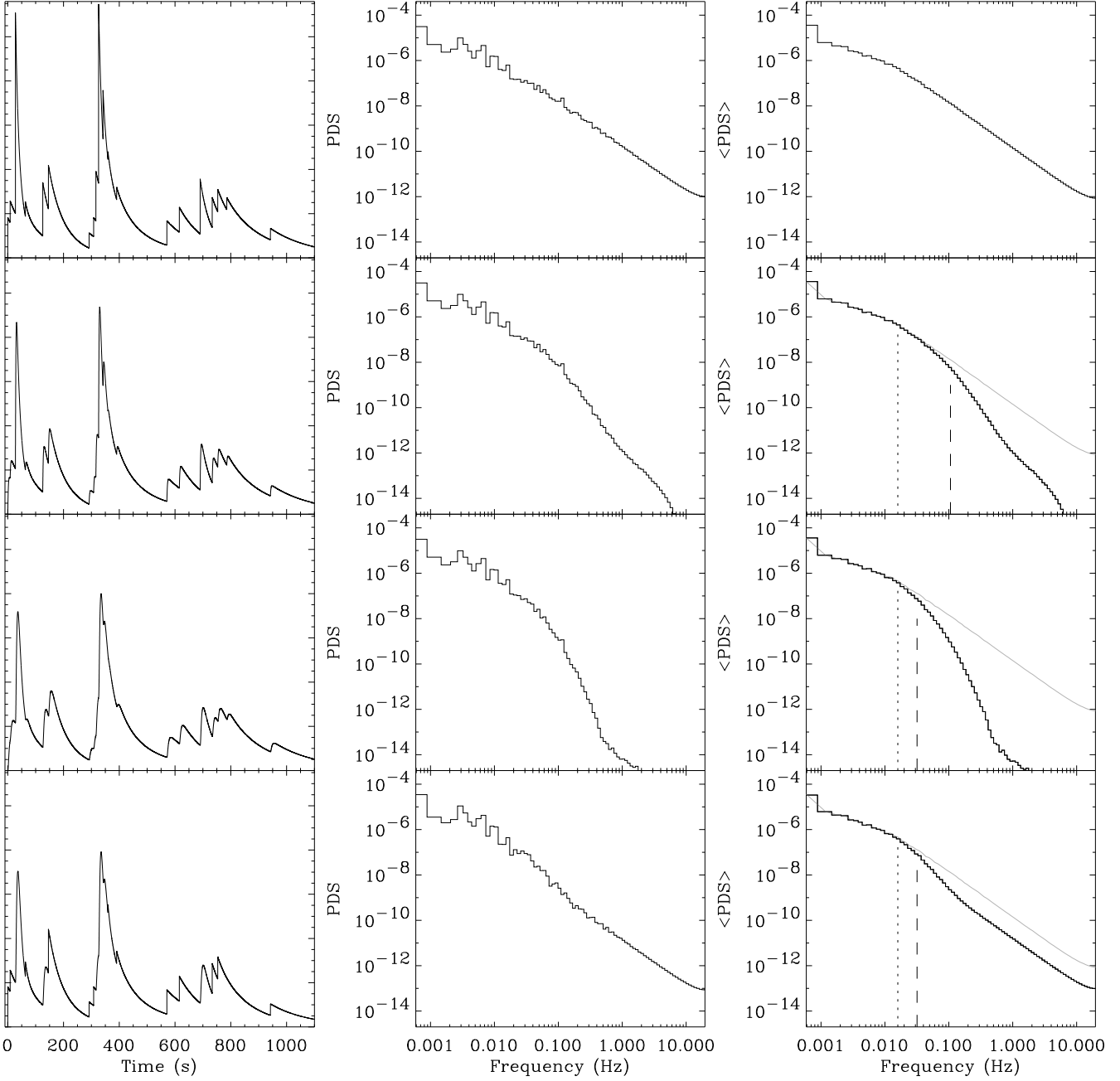


Figure 7. Simulated lightcurves and power spectra of a shot lightcurve with various degrees of scattering (see text for more details). The leftmost column shows the a sample simulated lightcurve, whose PSD is shown in the central column. The rightmost column shows the average PSD of 100 realizations of such a lightcurve. The first row show the case with no opacity and scattering. In the second row all the pulses are smeared by a scattering slab with $R\tau/c = 3$. In the third row all the pulses are smeared by a scattering slab with $R\tau/c = 10$. In the last row, the properties of the slab are held the same, but only the shortest pulses are smeared while the longest are unperturbed. In the rightmost column, the vertical dashed line shows the position of the scattering break, the vertical dotted line shows the position of the pulse break and the gray line show the unscattered average spectrum of the uppermost row. All the simulations are made by single exponential shots (**Eq. 7**) and contain 20 pulses. The pulse fluence has a log-normal distribution, while the pulse duration τ_d is distributed according to Eq. 8 with $a = -1/2$, $\alpha_m = 10$ s and $\alpha_M = 250$ s.

not be scattered with the same value of $\tau R/c$ since the shortest pulses are likely to be produced closer to the engine, where the relativistic wind is more dense and opaque. To mimic such a case, we consider a lightcurve in which only the shortest pulses underwent scattering. In this case, the PSD should show a steepening break followed by a flatten-

ing break when the unscattered pulse component becomes dominant (see lowest right panel of Fig. 7). Again, this is not observed in real data (see Fig. 2).

It may be argued that these models are too simplistic, since in real simulations each pulse is smeared with its own value of the parameter $\tau R/c$. What emerges from our anal-

ysis is that no clear signature of scattering is present in the PSD data. It may still be possible that a more detailed numerical simulation for the evolution of the flow can include scattering in such a way that its effect is relevant but does not produce a cutoff in the PSD. This requires however a fine tuning of the distribution of the parameter $\tau R/c$ and that the shape of at least part of the pulses is dominated by the transfer functions of Fig. 5. Such simulations, with a proper treatment of the scattering, are called for if the proposed link between scattering and variability has to be believed.

Even though scattering processes are shown to be not important in determining the variability parameter V , it is still possible that they have some relevance in shaping the spectra of GRBs. In fact, if the scattering screen is small and thick, the cutoff frequency can be large, in a range in which the PSD is dominated by the white noise. This kind of scattering would not be influential for the temporal pulse profile, but the photon energy may be shifted by

$$\Delta\epsilon \simeq \frac{\tau^2 \epsilon}{m_e c^2} (4kT - \epsilon) \quad (17)$$

where T is the temperature of the scattering electrons. This mechanism for modifying the typical energy of the photons in GRB spectra has been proposed and discussed, e.g., in Ramirez-Ruiz & Lloyd-Ronning (2002) and Mészáros et al. (2002). In particular, assuming that the comoving electron temperature is small and asking that the photon energy is sizably modified ($\Delta\epsilon \sim \epsilon$) one can show that the opacity must be

$$\tau \sim \sqrt{\frac{m_e c^2}{\epsilon}} \approx \sqrt{\Gamma} \quad (18)$$

where Γ is the bulk Lorentz factor of the flow and the right-most term holds if the initial observed energy of the photon was closed to $m_e c^2$.

Before discussing this issue in detail, we consider that all the computation described above are relevant if the scattering screen is comoving with the relativistic flow. In fact, in order to preserve the burst variability, a scattering screen at rest in the frame of the host galaxy needs to have an optical depth much smaller than unity. For this reason, the screens that we consider here are comoving with the flow, they can be the same shell in which the radiation is produced, or the total contribution of previously ejected shells.

In order for the scattering to be important in shaping the spectrum of GRBs, one has to assume a large opacity, so that the cutoff in the power spectrum should be exponential. Consider the bursts with largest variability (lower left panel of Fig. 2). The spectrum is well described by a power-law up to observed comoving frequencies $\nu \sim 10$ Hz. We can then constrain the comoving size of the scattering screen to be

$$R' < 10^9 \Gamma^{1/2} \quad (19)$$

In the framework of internal shock, the comoving width of the shell is given by $\Delta' = r/\Gamma \sim r_0\Gamma$, where r_0 is the size of the shell at the moment of the ejection. The constraint 19 implies then

$$r_0 \lesssim 10^8 \Gamma_2^{-1/2} \quad (20)$$

which is consistent with the internal shock picture only if the inner engine produces many shells, of the order of 1000

shells in a burst lasting for 10 seconds. Without being confined in the standard internal shock model, one can envisage a scenario in which the energy is liberated in the fireball at radii $r < r_0\Gamma^2$. In this case, it must be considered that the photons will be advected by the flow, which will become optically thin to radiation (due to the shell expansion) in a time scale smaller than the diffusion time scale of the photons. In this case, the break frequency would be expected to be at $\nu \simeq c\Gamma^2/(2\pi R)$, which is always above the measured 10 Hz.

7 CONCLUSIONS

We have computed the average power spectrum density for a set of GRB lightcurves, divided in 6 bins according to their variability properties and we have developed a shot noise model to be compared with them. Photon scattering is self consistently included in the model. We find that:

- The variability parameter V as computed by Fenimore & Ramirez-Ruiz (2000) strongly correlates with the dominant frequency of the spectra, being defined as the maximum of the $\nu PSD(\nu)$ function. This frequency is relatively small, suggesting that the luminosity of GRBs is related to the variability properties of the lightcurve in the low frequency range ($0.1 \div 10$ s).
- The average power spectra are well described by broken power laws with low frequency slope $\nu^{-2/3}$ and high frequency slope ν^{-2} . The break frequency is a function of the variability parameter V .
- The PSDs can be easily interpreted as due to the superposition of random similar shots (with a distribution of decay times and fluences) with double exponential shape (possibly stretched, see Norris et al. 1996). In this case the position of the break frequency (and therefore the variability parameter V) is related to the shortest relevant pulses in the duration distribution of pulses.
- We show that photon scattering should imprint a detectable break or cutoff in the PSD. The lack of such a signature makes untenable all models in which the luminosity variability correlation is ascribed to the smoothing of the shortest time scales in low-luminosity GRBs.
- Under certain circumstances (a compact engine or deviations from the standard internal shock picture) it is possible to find models in which photon scattering plays a relevant role in shaping the spectra of GRBs consistent with the measured PSD.

To conclude, it must be emphasized that the results we have presented do depend at some level on the existence of a tight correlation between the burst variability and luminosity. In particular, all the spectral analysis is made on the *rest frame frequency*, which is calculated thanks to the redshift guessed from the above mentioned correlation. However, the results still are valid and relevant even if such correlation should be proved not to be real. In that case, the variability would not be related to the luminosity, but still we should conclude that scattering is not relevant in shaping the lightcurves of GRBs. To test this, we performed the same PSD analysis on the *observed frequencies*. The average spectral shapes do remain the same, even if the values of the brake frequencies are different and, again, there is no sign

of a cutoff that may indicate that scattering is relevant to determine the degree of variability of the lightcurves.

ACKNOWLEDGMENTS

I am indebted to Martin Rees and Luigi Stella for discussions and suggestions that stimulated and largely improved this work. I thank Enrico Ramirez-Ruiz for providing the variability data and for discussion on the variability luminosity correlation. I thank Andrei Beloborodov for discussions and for carefully reading this manuscript.

REFERENCES

- Beloborodov A. M., Stern B. E., Svensson R., 1998, *ApJ*, 508, L25 (B98)
- Beloborodov A. M., Stern B. E., Svensson R., 2000, *ApJ*, 535, 158 (B00)
- Chang H., Yi L., 2000, *ApJ*, 542, L17
- Chang H.-Y., Yoon S.-J., Choi C.-S., 2002, *A&A*, 383, L1
- Fenimore E. E., Ramirez-Ruiz E., 2000, *ApJ* submitted (astro-ph/0004176)
- Ghisellini G., Celotti A., Lazzati D., 2000, *MNRAS*, 313, L1
- Kobayashi S., Piran T., Sari R., 1997, *ApJ*, 490, 92
- Kobayashi S., Ryde F., MacFadyen A., 2002, *ApJL* in press (astro-ph/0110080)
- Lazzati D., Stella L., 1997, *ApJ*, 476, 267 (LS97)
- Leahy D. A., Darbro W., Elsner R. F., Weisskopf M. C., Kahn S., Sutherland P. G., Grindlay J. E., 1983, *ApJ*, 266, 160
- Li H., Fenimore E. E., 1996, *ApJ*, 469, L115
- Lloyd-Ronning N. M., Fryer C. L., Ramirez-Ruiz E., 2002, *ApJ*, 574, 554
- Lloyd-Ronning N. M., Ramirez-Ruiz E., 2002, *ApJ*, 576, 101
- McBreen B., Hurley K. J., Long R., Metcalfe L., 1994, *MNRAS*, 271, 662
- Mészáros P., Rees M. J., 2000, *ApJ*, 530, 292
- Mészáros P., Ramirez-Ruiz E., Rees M. J., Zhang B., 2002, *ApJL* in prss (astro-ph/0205144)
- Norris J. P., Nemiroff R. J., Bonnell J. T., Scargle J. D., Kouveliotou C., Paciesas W. S., Meegan C. A., Fishman G. J., 1996, *ApJ*, 459, 393
- Norris J. P., Marani G. F., Bonnell J. T., 2000, *ApJ*, 534, 248
- Panaitescu A., Spada M., Mészáros P., 1999, *ApJ*, 522, L105
- Ramirez-Ruiz E., Fenimore E. E., 2000, *ApJ*, 539, 712
- Ramirez-Ruiz E., Lloyd-Ronning, L. M., 2002, *New Astronomy*, 7, 197
- Rees M. J., Mészáros P., 1994, *ApJ*, 430, L93
- Reichart D. E., Lamb D. Q., Fenimore E. E., Ramirez-Ruiz E., Cline T. L., Hurley K., 2001, *ApJ*, 552, 57
- Salmonson J. D., 2000, *ApJ*, 544, L115
- Spada M., Panaitescu A., Mészáros P., 2000, *ApJ*, 537, 824
- Spada M., Ghisellini G., Lazzati D., Celotti A., 2001, *MNRAS*, 325, 1559